International Journal of Scientific Research in Engineering and Management (IJSREM)
Volume: 10 Issue: 03 | March - 2026 SJIF Rating: 8.659 ISSN: 2582-3930

Green Synthesis, Characterization and Application of MnO_2 and Cr2O3 Nanoparticles Using Calotropis gigantea Plant Extract

V. Shanthi[1] G. Savari Susila [2]

[1] M.Sc Chemistry, Department of Chemistry, St. Mary's College (Autonomous) Affiliated to Manonmaniam Sundaranar University, Thoothukudi–628001, Tamilnadu, India.
[2] Assistant Professor, Department of Chemistry, St. Mary's College (Autonomous) Affiliated to Manonmaniam Sundaranar University, Thoothukudi–628001, Tamilnadu, India.

Abstract : This study focuses on the green synthesis of manganese dioxide (MnO_2) and chromium oxide (Cr_2O_3) nanoparticles using *Calotropis gigantea* leaf extract as a natural reducing and stabilizing agent, providing an eco-friendly, cost-effective, and sustainable approach. The synthesized nanoparticles were characterized using UV–Visible, FT-IR, XRD, FE-SEM, EDAX, and thermal analysis, confirming successful formation with high purity, good crystallinity, and spherical to quasi-spherical morphology in the size range of 20–50 nm. The presence of metal–oxygen bonds and plant-derived functional groups was also verified, along with good thermal stability. Antibacterial studies showed moderate activity against both Gram-positive and Gram-negative bacteria, with MnO_2 being more effective against Gram-negative strains and Cr_2O_3 against Gram-positive strains. Corrosion studies indicated that nanoparticle coatings significantly improved the corrosion resistance of mild steel, with Cr_2O_3 exhibiting superior inhibition efficiency. Overall, Cr_2O_3 nanoparticles demonstrated better antibacterial and anticorrosion performance, highlighting their potential applications in protective coatings, environmental remediation, and biomedical fields.

Key Words: Green synthesis, MnO_2 nanoparticles,Cr_2O_3 nanoparticles,Antibacterial activity,Corrosion inhibition

INTRODUCTION

ManganeseDioxide(MnO_2)Nanoparticles

MnO_2 nanoparticles synthesized through green methods offer an eco-friendly, cost-effective, and biocompatible alternative to conventional techniques. They possess unique structural and catalytic properties, making them highly useful in various fields. These nanoparticles exhibit strong photocatalytic activity for degrading organic dyes and show effective antimicrobial action against both Gram-positive and Gram-negative bacteria through reactive oxygen species (ROS) generation. They are also widely applied in water purification due to their high adsorption capacity. In energy applications, MnO_2 nanoparticles act as efficient catalysts in water splitting and are promising materials for supercapacitors because of their high capacitance and fast ion transport. In the biomedical field, they function as drug carriers, biosensors, and therapeutic agents, particularly in cancer treatment, where they enhance imaging and therapy. Their nanoscale size (1–100 nm), multiple crystal structures, and high redox activity further contribute to their versatility in environmental, energy, and medical applications[1].

ChromiumOxide(Cr_2O_3)Nanoparticles

Cr_2O_3 nanoparticles prepared via green synthesis are environmentally friendly materials known for their excellent thermal stability, corrosion resistance, and catalytic properties. They are effective photocatalysts for

degrading pollutants and exhibit strong antimicrobial activity through ROS generation. These nanoparticles are widely used in wastewater treatment for removing dyes and heavy metals. Additionally, Cr_2O_3 nanoparticles serve as catalysts in redox reactions and are explored as electrode materials in supercapacitors, especially when combined with conductive materials. With particle sizes typically ranging from 10–100 nm, they possess a stable rhombohedral structure and strong chemical resistance. Their applications extend to pigments, coatings, sensors, and energy storage systems, making them valuable in industrial and environmental fields[2].

2. MATERIALS AND METHODS

BIOSYNTHESIS OF MANGANESE DIOXIDE AND CHROMIUM OXIDE NANOPARTICLES USING *CALOTROPIS GIGANTEA* PLANT Collection of Plant

Fresh leaves of *Calotropis gigantea* were collected from healthy plants growing naturally in the college ground. The collection site was free from industrial activities, sewage disposal, and heavy vehicular traffic to avoid environmental contamination. The collected leaves were thoroughly washed with running tap water to remove dust and surface impurities, followed by rinsing with double distilled water. The cleaned leaves were then shade-dried at room temperature for 7–10 days to preserve thermolabile and bioactive phytochemical constituents. The dried leaves were subsequently used for the preparation of plant extract for the biosynthesis of manganese dioxide nanoparticles.

Fig -1 Image of Collecting of plant

Preparation of Calotropis gigantea Leaf Extract

The shade-dried leaves of Calotropis gigantea were ground into a fine powder using a blender and stored in airtight containers at room temperature away from direct sunlight. About 5 g of the powdered leaf material was transferred into a clean beaker containing 100 mL of distilled water. The mixture was heated and gently boiled at 60–80 °C for 20–30 minutes with continuous stirring to ensure uniform extraction of bioactive phytochemicals. After boiling, the extract was allowed to cool to room temperature and then filtered through Whatman No. 1 filter paper. The clear filtrate obtained represented the aqueous leaf extract, which was collected and stored in airtight containers at 4 °C and used for further biosynthesis of manganese dioxide nanoparticles.

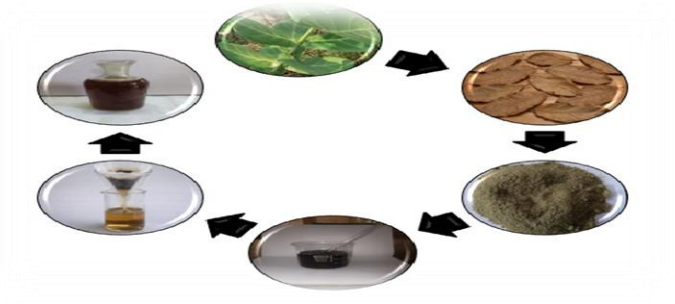

Fig -2 Schematic representation of the Preparation of Calotropis gigantea Leaf Extract

Synthesis of Manganese dioxide Nanoparticles

50 mL of 0.1 M manganese acetate tetrahydrate was taken in a beaker. 100 mL of plant extract was added

to the prepared manganese acetate tetrahydrate solution. The reaction mixture was heated at 80 °C for 2 hours using a magnetic stirrer. During heating, the solution colour changed from light brown to dark brown, indicating the reduction process and formation of manganese oxide precursor. After the colour change, 0.1 M NaOH solution was added dropwise under constant stirring to adjust the pH to around 10–11, which promotes complete precipitation and formation of manganese dioxide (MnO_2) nanoparticles.The mixture was then filtered using Whatman No. 1 filter paper. The filtrate was dried in a hot air oven until complete evaporation of water. The obtained dried powder was calcined in a muffle furnace at 400–500 °C for 2–3 hours, resulting in the formation of MnO_2 nanoparticles. The synthesized MnO_2 powder was stored in airtight containers for further characterization and application studies. Similarly to other metal chromium oxide.

3. RESULT AND DISCUSSIONS

Ultraviolet -Visble Spectroscopy

UV analysis of MnO_2 - G

The UV–Visible absorption spectrum of MnO_2-G nanoparticles was recorded in the range of 200–1100 nm. A strong absorption peak observed around 270–280 nm corresponds to band-to-band electronic transitions, confirming the successful formation of MnO_2 nanoparticles. A weak and broad peak in the region of 390–410 nm is attributed to surface defects, oxygen vacancies, or localized energy states within the band gap.

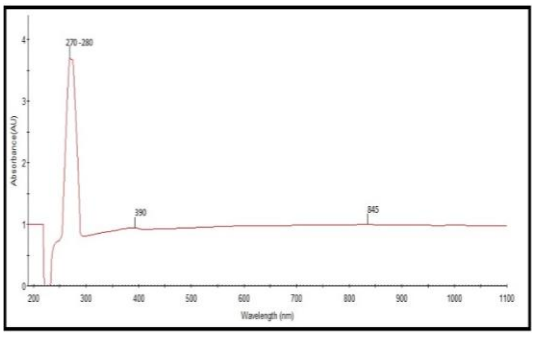

Fig-3 Image of UV-Visible absorption spectrum of Cr_2O_3 - G Nanoparticles

Additionally, a low-intensity absorption band near 800–850 nm is associated with defect-related or d–d electronic transitions [3]. The absence of significant peaks in the visible region indicates good optical purity and minimal impurities. Overall, the UV–Visible analysis confirms the optical properties of MnO_2 nanoparticles, highlighting their potential for photocatalytic, optoelectronic, and sensing applications.

UV analysis of Cr_2O_3 - G

The UV–Visible absorption spectrum of Cr_2O_3-G nanoparticles was recorded in the range of 200–900 nm. A strong absorption peak around 270 nm is attributed to band-to-band or charge transfer transitions, confirming the formation of Cr_2O_3 nanoparticles. Another peak near 366 nm is associated with defect states or localized energy levels within the band gap.

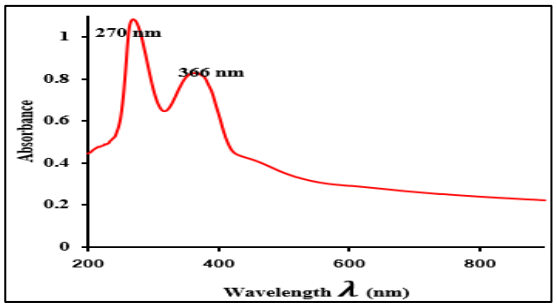

Fig-4 Image of UV-Visible absorption spectrum of Cr_2O_3 - G Nanoparticles

The gradual decrease in absorbance toward the visible and near-infrared regions indicates good optical purity with minimal impurities. The absorption in the near-visible region enhances light-harvesting ability, making the material suitable for photocatalytic, optoelectronic, and sensing applications[4].

Fourier Transform – Infrared Spectroscopy (FT-IR)

FT-IR anlaysis of MnO_2 – G

The FT-IR spectrum of green-synthesized MnO_2 nanoparticles shows characteristic peaks confirming their formation. Strong absorption bands in the 400–700 cm^{-1} region correspond to Mn–O stretching vibrations, indicating the formation of the MnO_2 lattice. A broad peak around 3400 cm^{-1} is attributed to O–H stretching of surface hydroxyl groups, while the band near 1600 cm^{-1} corresponds to bending vibrations of adsorbed water molecules.

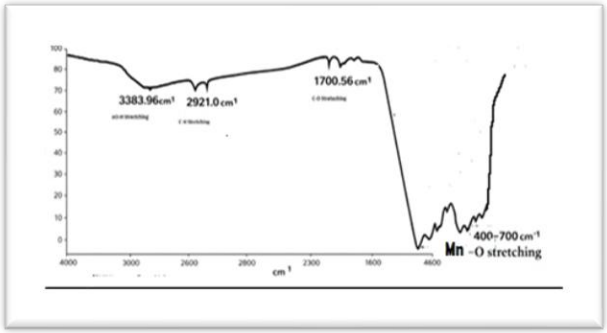

Fig-5 Image of FTIR spectrum of MnO_2 - G nanoparticles

These hydroxyl and water-related peaks are typical in green synthesis and arise from moisture adsorption and plant-derived phytochemicals acting as reducing and stabilizing agents. Overall, the FT-IR results confirm the successful formation of MnO_2 nanoparticles with surface functional groups, demonstrating the effectiveness of the green synthesis method[5].

FTIR analysis of Cr_2O_3 – G

The FTIR spectrum of the synthesized Cr_2O_3 nanoparticles shows characteristic peaks confirming the formation of chromium oxide. Strong absorption bands in the 400–700 cm^{-1} region are attributed to Cr–O stretching vibrations, indicating the formation of the metal oxide structure. A broad peak around 3400 cm^{-1} corresponds to O–H stretching vibrations, suggesting the presence of surface hydroxyl groups and hydrogen-bonded water molecules.

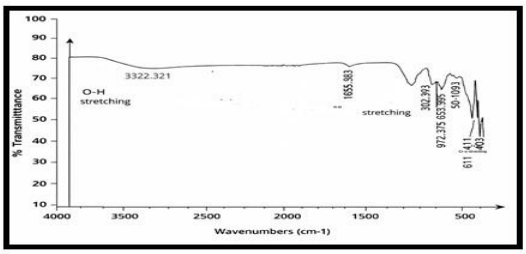

Fig- 6 Image of FTIR spectrum of Cr_2O_3 -G Nanoparticles

The band near 1600 cm^{-1} is assigned to H–O–H bending vibrations of adsorbed water. Although slight variations in peak positions may occur due to synthesis conditions, the presence of Cr–O and O–H bands confirms the successful formation of Cr_2O_3 nanoparticles with surface hydroxyl functionalities, consistent with reported studies[6].

X-ray Diffraction (XRD)

XRD analysis of MnO_2 – G

The X-ray diffraction (XRD) pattern of green-synthesized MnO_2 nanoparticles confirms the formation of crystalline MnO_2 with a tetragonal structure (β-MnO_2). The observed diffraction peaks at various 2θ values correspond to characteristic crystallographic planes and match well with standard JCPDS data (No. 44-0141), indicating successful phase formation and structural purity. The absence of impurity peaks suggests high phase homogeneity of the synthesized nanoparticles.

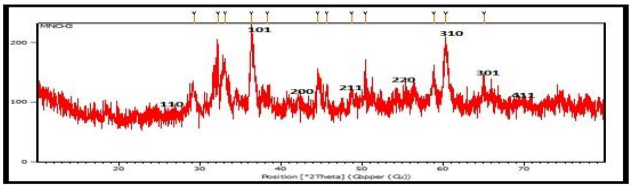

Fig- 7 Image of XRD spectrum of Mno_2 -G Nanoparticles

The sharp and well-defined peaks indicate good crystallinity, while peak broadening confirms the nanoscale size of the particles. The calculated crystallite size using the Debye–Scherrer equation falls within the nanometer range, which is typical for green synthesis methods. Overall, the XRD results validate the successful synthesis, structural stability, and high purity of MnO_2 nanoparticles [7].

XRD analysis of Cr_2O_3 – G

The XRD pattern of green-synthesized Cr_2O_3 nanoparticles confirms the formation of a well-crystallized rhombohedral α-Cr_2O_3 phase. The observed diffraction peaks at various 2θ values correspond to characteristic crystallographic planes and match well with standard JCPDS data (No. 38-1479), indicating successful phase formation. The nanoparticles crystallize in a trigonal crystal system (space group R-3c) with lattice parameters close to standard values, confirming structural stability.

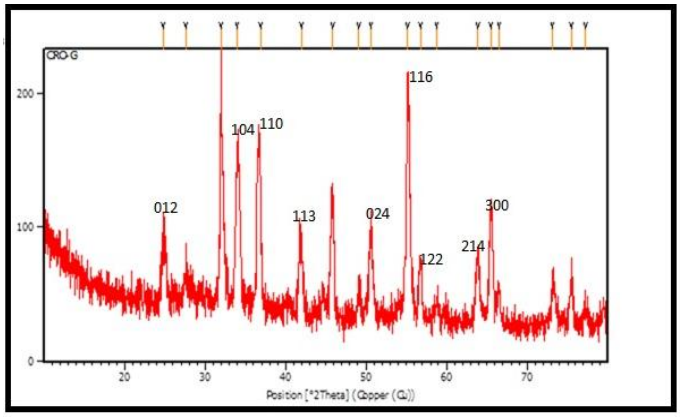

Fig-8 Image of XRD spectrum of Cr_2O_3 – G Nanoparticles

The absence of impurity peaks indicates high purity of the synthesized material. Sharp and intense peaks suggest good crystallinity, while peak broadening confirms the nanoscale nature of the particles. The average crystallite size, calculated using the Debye–Scherrer equation, is around 27.9 nm. Overall, the XRD results validate the successful synthesis, phase purity, and nanocrystalline nature of Cr_2O_3 nanoparticles[8].

Field Emission Scanning Electron Microscope (FE-SEM)

FE-SEM analysis of MnO_2 – G

Scanning Electron Microscopy (SEM) analysis of the green-synthesized MnO_2 nanoparticles reveals predominantly spherical to quasi-spherical particles with a fairly uniform distribution, indicating effective stabilization by plant-derived phytochemicals. The particle size ranges from 20–50 nm, confirming their nanoscale nature. Slight agglomeration is observed due to high surface energy and interparticle interactions, which is common in biologically synthesized nanoparticles.

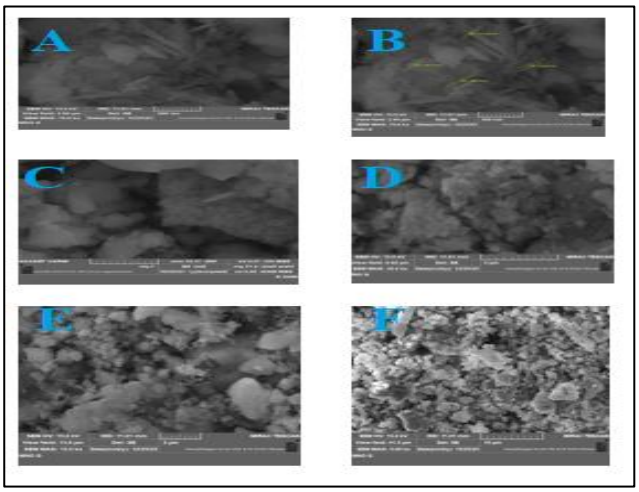

Fig -9 Images of FE-SEM images of MnO_2 nanoparticles

However, the absence of large bulk structures and the presence of well-defined particle boundaries indicate good crystallinity and structural stability, consistent with XRD results. Overall, the SEM analysis confirms that the green synthesis method produces MnO_2 nanoparticles with controlled morphology and suitable size for catalytic and antibacterial applications[9].

FE-SEM analysis of Cr_2O_3 – G

Scanning Electron Microscopy (SEM) analysis of the green-synthesized Cr_2O_3 nanoparticles shows predominantly spherical to quasi-spherical particles with slight irregularity and moderate agglomeration. The particle size ranges between 20–50 nm, confirming their nanoscale formation. The observed aggregation is due to high surface energy and interparticle interactions, which are common in green-synthesized nanoparticles.

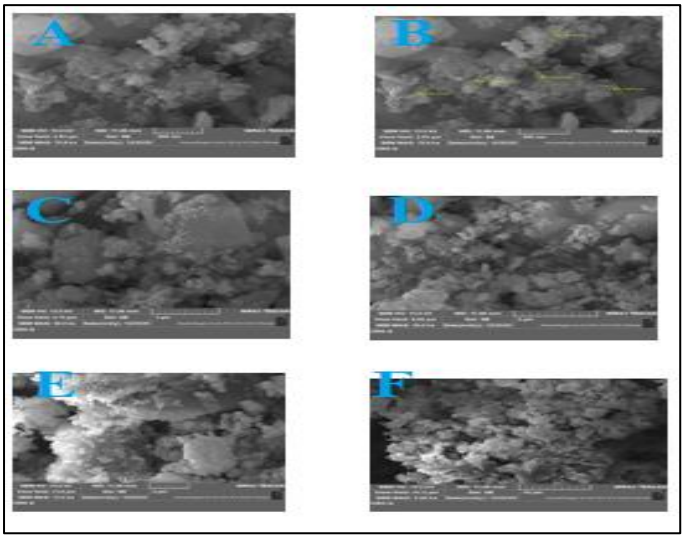

Fig -10 Images of FE-SEM images of MnO_2 nanoparticles

The particles are well-defined without large bulk structures, indicating good crystallinity and structural stability, consistent with XRD results. Additionally, the rough and porous surface enhances the surface area, making the nanoparticles suitable for catalytic and antibacterial applications. Overall, the SEM results confirm that the green synthesis method effectively produces Cr_2O_3 nanoparticles with controlled morphology and nanoscale size[9].

Energy Dispersive X-ray Analysis (EDAX)

EDAX analysis of MnO_2- G

Energy Dispersive X-ray (EDAX) analysis of the green-synthesized MnO_2 nanoparticles confirms their elemental composition. The spectrum shows prominent peaks corresponding to manganese (Mn) and oxygen (O), verifying the formation of MnO_2. The oxygen peak around 0.52 keV is attributed to the O Kα transition, while manganese peaks near 5.9 keV and 6.5 keV correspond to Mn Kα and Mn Kβ transitions.

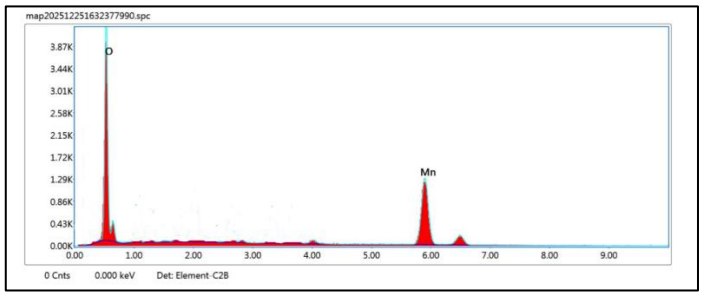

Fig-11 Images of EDAX Analysis of MnO_2 nanoparticles

The absence of additional peaks indicates that the nanoparticles are free from impurities, demonstrating high purity achieved through the green synthesis method. Overall, the EDAX results confirm the successful formation, purity, and chemical stability of MnO_2 nanoparticles, consistent with reported studies[9].

EDAX analysis of Cr_2O_3 -G

Energy Dispersive X-ray (EDAX) analysis of the green-synthesized Cr_2O_3 nanoparticles confirms their elemental composition. The spectrum shows strong peaks corresponding to chromium (Cr) and oxygen (O), verifying the formation of Cr_2O_3. The oxygen peak around 0.5 keV is attributed to the O Kα transition, while chromium peaks near 5.4 keV and 5.9 keV correspond to Cr Kα and Cr Kβ transitions.

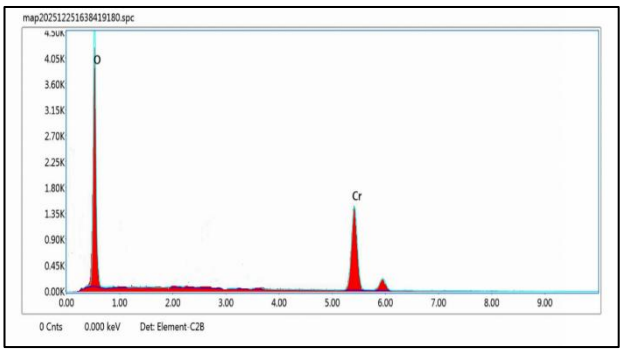

Fig-12 Images of EDAX Analysis of Cr_2O_3 -G nanoparticles

The absence of additional peaks indicates high purity of the synthesized nanoparticles with no detectable impurities. Overall, the EDAX results confirm the successful formation, purity, and stability of Cr_2O_3 nanoparticles, demonstrating the effectiveness of the green synthesis method [9].

Combined TG- DTA-DTG Mno2-G

Thermogravimetric (TG), DTG, and DTA analyses of green-synthesized MnO_2 nanoparticles were performed up to 900 °C to evaluate thermal stability. A small weight loss below 120 °C is due to moisture removal, while a second loss between 150–350 °C corresponds to the decomposition of residual organic compounds from the synthesis process. The DTG curve shows a peak in this region, indicating the rate of decomposition.

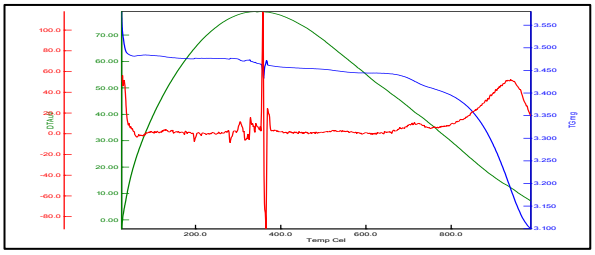

Fig-13 TG-DTA-DTG Curve of Mno2-G Nanoparticles

A stable region from 350–600 °C confirms good thermal stability, and slight changes above 600 °C are related to phase transformation and structural rearrangement. The DTA curve further supports these changes through endothermic and exothermic peaks. Overall, the results indicate that MnO_2 nanoparticles exhibit good thermal stability for various applications[10].

Combined TG- DTA-DTG Cr2o3-G

TG, DTG, and DTA analyses of green-synthesized Cr_2O_3 nanoparticles show good thermal stability up to 900 °C. A small weight loss below 150 °C is due to moisture removal, while the loss between 150–350 °C is attributed to the decomposition of residual organic compounds.

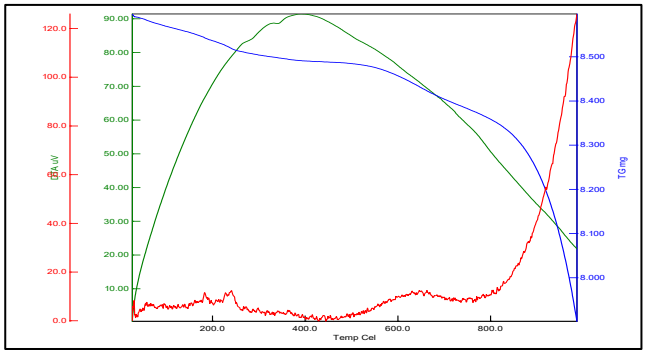

Fig-14TG-DTA-DTG Curve of Cr_2O_3 -G Nanoparticles

A stable region from 350–600 °C confirms the formation of stable Cr_2O_3 nanoparticles. Above 600 °C, minimal weight change occurs due to structural rearrangement and improved crystallinity. Overall, the results indicate excellent thermal stability, making the nanoparticles suitable for high-temperature applications[10].

Analysis of TGA of Mno2- G

Thermogravimetric analysis (TGA) of the sample shows a total weight loss of 13.2% from room temperature to 1000 °C. An initial loss of 4.7% between 100–350 °C is attributed to the removal of adsorbed moisture and volatile components. The sample remains relatively

stable between 350–600 °C with minimal weight change, indicating good thermal stability.

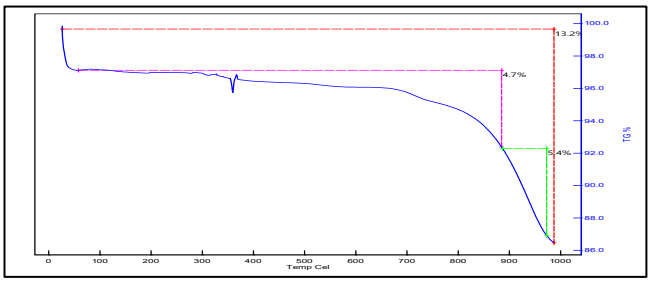

Fig- 15 TGA Curve of Mno2- G Nanoparticles

A further weight loss of 5.4% from 600–950 °C is associated with the decomposition of the main matrix or organic constituents. At 1000 °C, about 86.8% residue remains, confirming the presence of thermally stable inorganic material. Overall, the sample exhibits good stability up to 600 °C, with significant decomposition at higher temperatures[10].

Analysis of TGA Cr2o3 -G

Thermogravimetric analysis (TGA) of the green-synthesized Cr_2O_3 nanoparticles was performed up to 1000 °C to assess thermal stability. A small weight loss of about 2% below 200 °C is attributed to the removal of adsorbed moisture and surface water. A gradual weight loss between 200–750 °C corresponds to the decomposition of plant-derived organic compounds used during synthesis.

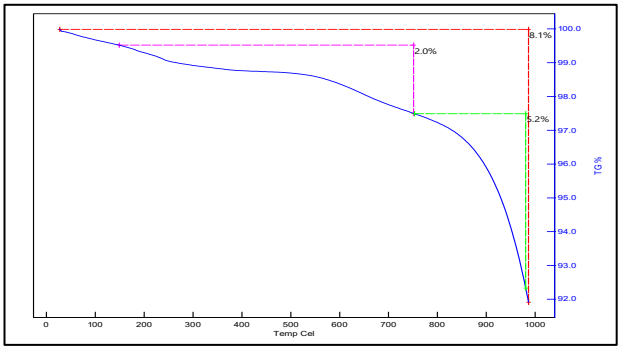

Fig- 16 TGA Curve of Cr_2O_3 - G Nanoparticles

A further weight loss of around 5.2% above 750 °C is associated with the degradation of remaining organic residues and structural rearrangement of the nanoparticles.Overall, the total weight loss of approximately 8.1% indicates good thermal stability, confirming the formation of stable Cr_2O_3 nanoparticles with minimal organic impurities[10].

ANTIBACTERIAL ACTIVITY

The antibacterial activity of green-synthesized CrO-G and MnO-G nanoparticles was evaluated using the disc diffusion method against five bacterial strains: *Escherichia coli*, *Staphylococcus aureus*, *Bacillus subtilis*, *Bacillus cereus*, and *Klebsiella pneumoniae*, with ciprofloxacin as the standard. Ciprofloxacin showed strong activity (19–25 mm), while both nanoparticles exhibited moderate antibacterial effects.MnO-G showed relatively higher activity against *E. coli* (11 mm) and *Bacillus cereus* (10 mm), whereas CrO-G was more effective against *Bacillus subtilis* (9 mm). Moderate activity was observed against *Staphylococcus aureus*, and the lowest activity was recorded against *Klebsiella pneumoniae*.

TABULATION OF DIFFERENT BACTERIA

S.No	Name of Bacteria	Image
1	E. coli	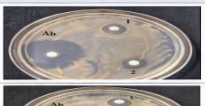
2	Staphylococcus aureus	
3	Bacillus subtilis	
4	Bacillus cereus	
5	*Klebsiella pneumoniae*	

The antibacterial effect is mainly due to reactive oxygen species (ROS) generation, membrane disruption, and interaction with cellular components.Overall, both nanoparticles demonstrate noticeable antibacterial

potential, with MnO-G being slightly more effective against Gram-negative bacteria and CrO-G against Gram-positive strains, though their activity is lower than the standard antibiotic.

Table : 1 Antibacterial activity of CrO-G, MnO-G

Bacteria	Inhibition zone in mm		
	Ab ciprofloxacin	1-CrO-G	2-MnO-G
E.coli	22	6	11
Staphylococcus aureus	25	7	6
Bacillus subtilis	24	9	8
Bacillus cereus	20	8	10
Kleibsiella pneumonia	19	5	7

ANTI-CORROSION ACTIVITY

The corrosion performance of MnO-G coated, CrO-G coated, and uncoated mild steel samples was studied in acidic, basic, and neutral environments using the weight loss method. The weight loss (ΔW) was calculated from the difference between initial (W_1) and final weight (W_2), and used to determine the corrosion rate.

The uncoated sample showed the highest corrosion rates in all media—1.41% in acid, 2.05% in base, and 1.54% in neutral—indicating its high vulnerability, especially in alkaline conditions.

Coating the metal with MnO-G significantly reduced the corrosion rate to 0.94% (acid), 1.60% (base), and 1.24% (neutral), demonstrating its protective effect.

The CrO-G coated sample exhibited the best performance, with the lowest corrosion rates of 0.60% (acid), 1.35% (base), and 0.38% (neutral), showing excellent resistance, particularly in neutral medium.

Inhibition Efficiency (%) $= \frac{CRuncoated - CRcoated}{CRuncoated} \times 100$

Table :2 Anti-corrosion efficiency (%) of MnO-G and CrO-G samples based on weight loss measurements in different media

Samples	Medium	W 1 (g)	W 2 (g)	ΔW (g)	Corrosion rate %
Mno-G	Acid	7.7123	7.6395	0.0728	0.94
	Base	7.6996	7.5764	0.1232	1.60
	Neutral	7.6241	7.5295	0.0946	1.24
Cro-G	Acid	7.7879	7.7407	0.0472	0.60
	Base	7.8219	7.7159	0.106	1.35
	Neutral	7.7531	7.7231	0.03	0.38
Uncoated	Acid	7.6819	7.5731	0.1088	1.41
	Base	7.7147	7.5565	0.1582	2.05
	Neutral	7.6933	7.5748	0.1185	1.54

Anti-Corrosion Efficiency

The anti-corrosion performance was evaluated by comparing coated samples with the uncoated metal. The MnO-G coating showed moderate inhibition efficiency, with values of 33.3% in acidic, 21.9% in basic, and 19.4% in neutral media. In contrast, the CrO-G coating demonstrated significantly higher efficiency, achieving 57.4% (acid), 34.1% (base), and 75.3% (neutral).

Among all conditions, the highest inhibition efficiency (75.3%) was observed for the CrO-G coating in neutral medium, indicating the formation of a strong and uniform protective film with better surface coverage.

The enhanced corrosion resistance of coated samples is attributed to the formation of a protective barrier layer, which prevents the interaction of corrosive ions with the metal surface, along with a possible passivation effect that reduces electrochemical reactions.

Table :3 Anti-corrosion efficiency (%) of MnO-G and CrO-G samples based on weight loss measurements in different media.

Samples	Medium	W3 (g)	W4 (g)	ΔW (g)	Anti corrosion activity of%
Mno-G	Acid	1.47	0.94	0.47	33.3
	Base	2.05	1.60	0.45	21.9
	Neutral	1.54	1.24	0.3	19.4
Cro-G	Acid	1.41	0.60	0.81	57.4
	Base	2.05	1.35	0.7	34.1
	Neutral	1.54	0.38	1.16	75.3

Overall, CrO-G coating outperformed MnO-G coating in all media, suggesting improved adhesion, stability, and surface protection. The neutral medium provided the best conditions for corrosion inhibition, while the basic medium was found to be the most aggressive.

4.CONCLUSIONS

The present study successfully synthesized MnO_2 and Cr_2O_3 nanoparticles using an eco-friendly green synthesis method with plant leaf extract, offering a cost-effective and sustainable approach. UV–Visible and FT-IR analyses confirmed the formation of nanoparticles with characteristic absorption peaks and metal–oxygen bonds along with surface functional groups. XRD results revealed that MnO_2 exhibited a tetragonal structure, while Cr_2O_3 showed a rhombohedral phase, both indicating high crystallinity and purity.

FE-SEM analysis demonstrated spherical to quasi-spherical morphology with particle sizes in the range of 20–50 nm, and EDAX confirmed their elemental composition. Thermal analysis (TG, DTG, and TGA) indicated good thermal stability of the synthesized nanoparticles. Antibacterial studies showed moderate activity against selected bacterial strains, with MnO–G being more effective against Gram-negative bacteria and CrO–G against Gram-positive bacteria, although both were less active than the standard antibiotic. Corrosion studies revealed that coated mild steel exhibited enhanced corrosion resistance, with CrO–G coating showing

superior performance and higher inhibition efficiency. Overall, Cr_2O_3 nanoparticles demonstrated better antibacterial and anticorrosion properties compared to MnO_2, highlighting their potential for applications in protective coatings, environmental remediation, and biomedical fields.

ACKNOWLEDGEMENT

I would like to express my gratitude to my primary supervisor, Dr.G.Savari Susila, who guided me throughout this Research article. I would also like to thank my friends and family who supported me and offered deep insight into the study.

REFERENCES

1. Devaraj, S., Munichandraiah, N.: Effect of crystallographic structure of MnO_2 on its electrochemical capacitance properties. *Journal of Physical Chemistry C* 112 (2008) 4406–4417.
2. Patil, S.S., Mali, M.G., Hong, C.K.: Green synthesis of chromium oxide nanoparticles and their applications in environmental remediation and energy storage. *Materials Letters* 201 (2017) 78–81.
3. Zhang, X., Li, H., Wang, Y., et al.: Optical and electrochemical properties of MnO_2 nanoparticles synthesized by green methods. *Journal of Alloys and Compounds* 509 (2011) 431–435.
4. Kumar, V., Singh, K., Kumar, A.: Optical properties of chromium oxide (Cr_2O_3) nanoparticles synthesized via green method. *Ceramics International* 42 (2016) 14420–14424.
5. Das, R., Bandyopadhyay, R., Pramanik, P.: Green synthesis of MnO_2 nanoparticles and their FT-IR characterization. *Materials Science in Semiconductor Processing* 41 (2016) 349–354.
6. Kumar, S., Kumar, A., Bahadur, D.: FT-IR and structural characterization of chromium oxide (Cr_2O_3) nanoparticles synthesized by green method. *Journal of Materials Science: Materials in Electronics* 27 (2016) 12345–12350.
7. Thackeray, M.M.: Structural considerations of layered and tunneled manganese oxides for electrochemical applications. *Progress in Solid State Chemistry* 25 (1997) 1–71.
8. Baghban, N., Momeni, S., Behboudi, E., et al.: Green synthesis and characterization of chromium oxide nanoparticles for environmental applications. *Materials Chemistry and Physics* 301 (2023) 127563.
9. Limaye, A.S., Rananaware, P., Ghosh, A., et al.: Greener synthesis of metal oxide nanoparticles and their morphological characterization. *ACS Applied Bio Materials* 7 (2024) 1790–1800.
10. Vyazovkin, S., Burnham, A.K., Criado, J.M., et al.:ICTACKineticsCommittee recommendations for performing kinetic computations on thermal analysis data. *Thermochimica Acta* 520 (2011) 1–19.